Generation of Windstorm in the Eastern Mountainous Coast of Korea

Choi Hyo[1*] and Choi Soo Min[2]
1. Dept. of Atmospheric Environmental Sciences, Gangneung-Wonju National University, Gangneung 210-702, KOREA
2. Konkuk University High School, 265 Guiro, Kwangjin-Gu, Seoul 143-853, KOREA
du8392@hanmail.net*

Abstract

Using a three-dimensional non-hydrostatic numerical model, WRF version 2.2, the evolution of windstorm was investigated near Mt. Taegulyang (alt. 896 m) located in 20 km west of a coastal city, Gangneung, Korea from October 27 through October 28, 2003. On October 27, before cold front passing across the Korean peninsula, no windstorm was detected in the study area and moderate southwesterly wind of 4 to 6 m/s prevailed in the study area. On the other hand, at 09 LST, October 28, just after the cold front passed by the coastal city, positive relative vorticity at 500 hPa level induced downward motion of cold air from the upper level toward the ground surface with a decreasing rate of air temperature of - 6 ^{0}C/day at 850 hPa level and simultaneously, negative geopotential tendency of - 160 m/day lay on the study area caused the atmospheric depth of 500 hPa level to be much shrunken vertically. These kinds of downward motion of cold air and compression of atmospheric depth resulted in merging of streamlines with higher speed more than 25 kts of isotach at 850 hPa level and produced the formation of strong surface wind speeds. As strong synoptic westerly wind blowing over the mountain toward the downwind side coastal city was associated with mountain-land breeze by both nocturnal cooling of the ground surface and steep mountain terrain, it could be an intensified strong downslope wind like Katabatic wind. Furthermore, as soon as synoptic westerly wind passed over the steep mountain barrier, a strong intensified downslope westerly wind depicted a cyclonic flow pattern to cause cyclogenesis in the downwind side and the wind speed increased, resulting in a good condition for the formation of a wind storm more than 9 m/s on the mountain and coastal surfaces. When this strong wind passed along the eastern slope of the mountain and by the coastal basin, it could be more enforced underneath much shallower nocturnal surface inversion layer than daytime convective boundary layer, showing more increase of its speed. As the centers of maximum positive vorticity and maximum negative geopotential tendency approached the coastal near noon on October 28, surface wind under the compressed atmospheric depth should be more intensified. Even though daytime convective boundary layer was developed with more increased depth than nocturnal surface inversion layer, the shrunken convective boundary layer under the strong downward motion of cold air behind cold front across the study area could still cause the increase of wind speed, resulting in daytime windstorm near noon in the study area. The windstorm in the lee side of the mountain displayed the propagation of internal gravity waves with a hydraulic jump motion bounding up and down over the coastal basin and sea such as blocking.

Keywords: Windstrom, Katabatic wind, Relative vorticity, Geopotential tendency, Cyclogensis, Mountain-land breeze, Convective boundary layer, Nocturnal surface inversion layer, Internal gravity waves, Hydraulic jump.

Introduction

The formation of severe windstorm in the mountainous coast is due to lee cyclogenesis associated with mesoscale convection and microphysical processes[1-5]. Lee cyclogenesis accompanying windstorm in the coast is generally detected when down slope motion of air is organized into jet like motion or the down slope motion exists over a steep terrain. Anderson[6] revealed katabatic wind field responding to nocturnal inversions in valleys, using a two-dimensional model. Pielke[7] also explained that windstorm in the mountain is generated by an intensified strong down slope wind like katabatic wind combined with synoptic scale wind and mountain-land breeze in the downwind side of a steep mountain. Hunt and Simpson[8] and Arya[9] depicted formation of internal gravity waves with a hydraulic jump in the lee side of the mountain in cases of different Froude numbers. Choi[10] also explained the formation of a down slope windstorm with internal gravity waves, depicting a hydraulic jump motion bounding up and down in the lee side of the mountainous coast of Korea by a three-dimensional numerical simulation and considered a windstorm to be a string wind over than 10 m/s.

Tropial cyclone called typhoon, hurricane and willy willy in Australia has an intense axisymmetric vortex about the vortex center and it has hazardous weather of strong winds more than 10 m/s, even 40 m/s in radical scales of several hundred kilometers[11-16]. Knauss[17] and

Choi[18] insisted that cyclonic surface winds also produces an intensive windstorm and in the coast, it induces upwelling of bottom cold waters on the sea surface, resulting in cold water outbreak in the coastal sea. The purpose of this study is to investigate the generation mechanism of windstorm, except for strong wind produced by tropical cyclone by numerical simulation using a three-dimensional model called WRF (Weather Research and Forecasting Model) - 2.2 and to predict the precursor of the development of windstorm in advance[19-20].

Study area

The study area around Gangneung city (K; $37^0$45N, $128^0$54E) indicating a fine-mesh domain (box) in fig. 1 covers an eastern part of Korean peninsula and its daily weather and climate are strongly affected by steep mountains and the East Korea Warm Current (EKWC) bound for north, following the eastern coast of Korea. The EKWC is branch current of Kuroshio Warm Current, which is a strong western boundary current in the western north Pacific Ocean and Kuroshio current begins off the east coast of Taiwan and flows northeastward past Japan, merging with the easterly drift of the North Pacific Current. The coastal sea near Gangneung city is more or less 100 m deep but 1 km away from the coast, the sea is deep greater than 100 m to 1000 m toward the east in the box domain (about 3800 m in the open sea).

As high mountainous area in the west is strongly heated during the day, upslope wind combined with valley wind from inland basin to the mountain top and sea breeze from the coast to the inland is generally developed, while nocturnal downslope wind combined with mountain-land breeze is dominant over the inland and coastal sea.

Numerical Method and Input Data

A three-dimensional, grid point Weather Research & Forecasting Model (WRF) version 2.2 model with a terrain following coordinate system was adopted for the generation of windstorm around Gangneung city (K; $37^0$45N, $128^0$54E) in the eastern mountainous coast of Korea for 48 hours numerical simulation from 0000 UTC (Local Standard Time (LST) = 9h + UTC; 0900 LST), October 27 through 0000 UTC, October 29, 2003. Through numerical simulation using the model, meteorological elements such as wind, temperature, potential temperature, relative humidity, relative vorticity, potential vorticity, streamline and 500 hPa height change for 24 hours (i.e. geopotential tendency ($\partial\Phi/\partial t$); m/day) were evaluated in northeastern Asia, Korean peninsula and near Gangneung city in the eastern coastal region of Korea. In the numerical simulation, one way, triple nesting process from a coarse-mesh domain to a fine-mesh domain was performed using a horizontal grid spacing of 27 km covering a 91 x 91 grid square in the coarse mesh domain and a 9 km interval also covering a 91 x 91 grid square in the second domain. The third domain through final nesting process consisted of a 3 km horizontal grid spacing again on a 91 x 91 grid square. NCEP/NCAR reanalysis FNL (1.0^0 x 1.0^0) data were used as meteorological input data to the model and was vertically interpolated onto 36 levels with sequentially larger intervals increasing with height from the surface to the upper boundary level of 100 hPa.

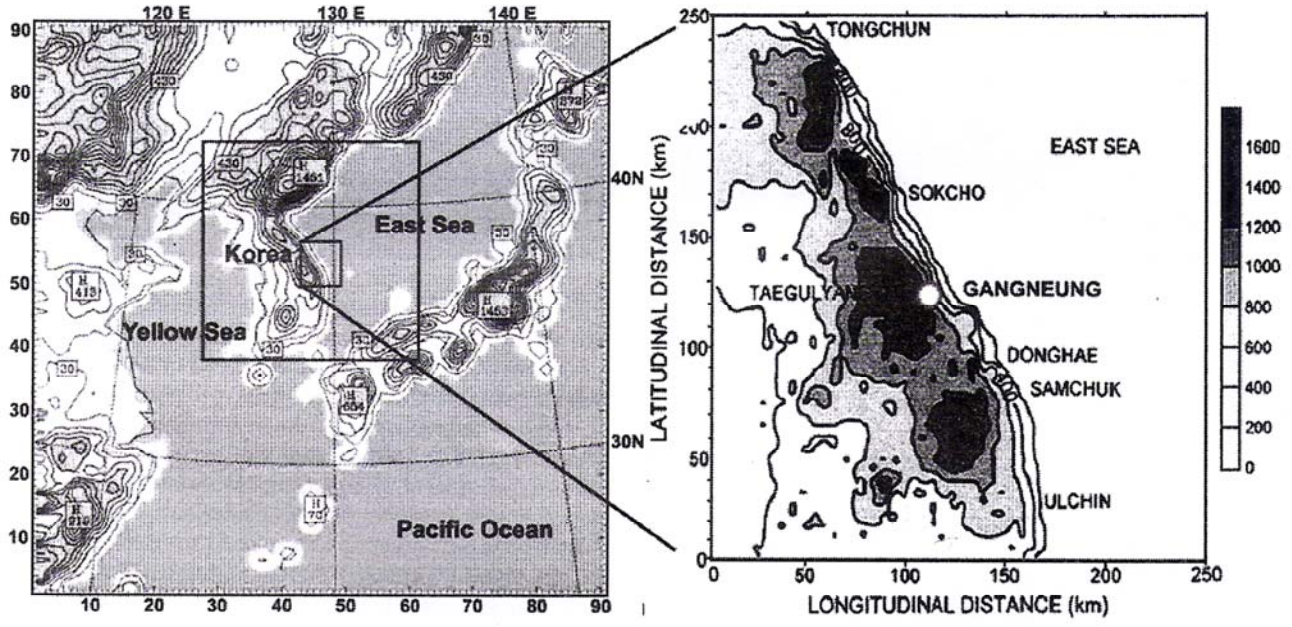

Figure 1: Topographical features in the vicinity of Korean peninsula in two coarse-mesh domains (horizontal resolutions of 27 km and 9 km) and the mountainous coastal region surrounding Gangneung city ($37^0$45N, $128^0$54E; 20 m above mean sea level) and Mt. Taegulyang (860 m) in a fine-mesh domain (horizontal resolution of 3km)

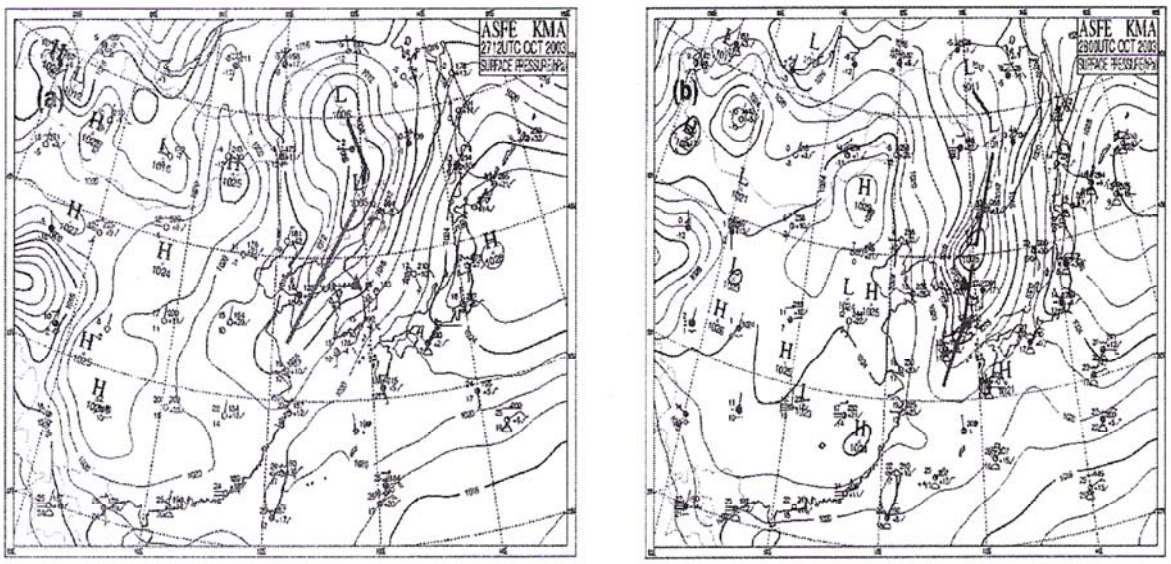

Figure 2: Surface weather maps at (a) 2100 LST, October 27, 2003 and (b) 0900 LST, October 28 (two hours before windstorm occurrence at Gangneung). Thick line passing through low pressure center and triangle denotes cold front and Gangneung city of Korea

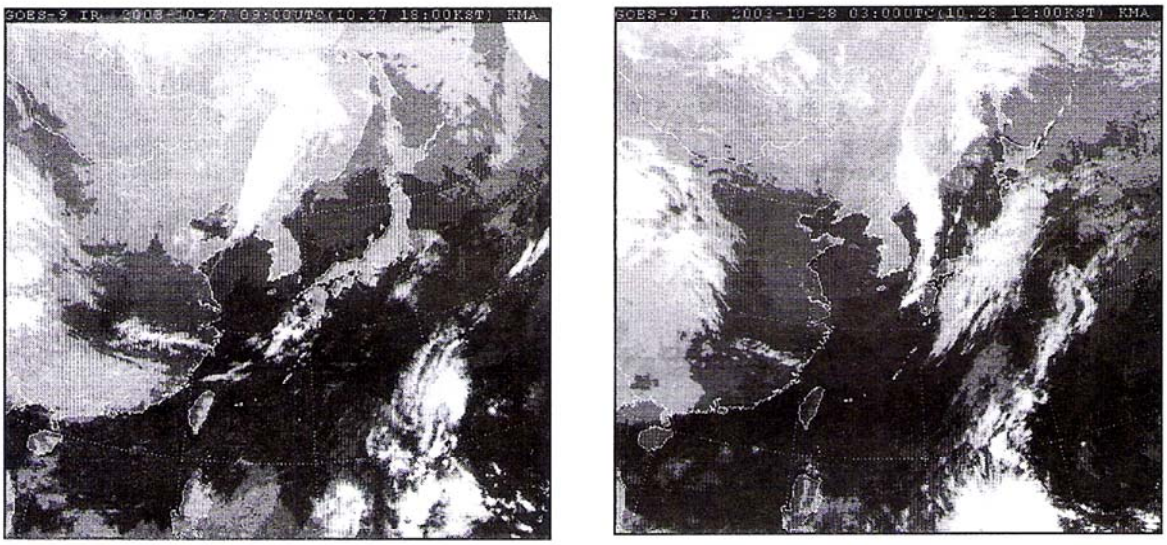

Figure 3: GOES-9 IR satellite images (a) 1800 LST, October 27, 2003 (moderate wind) and (b) 1200 LST, October 28 (windstorm occurrence near Gangneung). Thick white bands in the northwestern Korean peninsula extending to a low pressure center in (a) and from north near Vladivostok of Russia to south near Kyusu Island of Japan in the East Sea of Korea in (b) denote cold fronts.

For the heat and moist budgets in the atmospheric boundary layer, the WSM 6 scheme was used for microphysical processes and the YSU PBL scheme for the planetary boundary layer. The Kain-Fritsch (new Eta) for cumulus parameterization, the five thermal diffusion model for land surface and the RRTM long wave radiation scheme and dudhia short wave radiation schemes were also used. For calculating 3 hours accumulated precipitation amount, a mixed phase of both ice and water was considered. Hourly archived wind, air temperature, relative humidity, cloud and geopotential tendency by Gangwon Regional Meteorological Administration were used for the verification of numerical results of the meteorological elements. In addition, GMS-IR satellite images made by the Japan Meteorological Agency were used for chasing cold front and obtaining cloud information.

Results and Discussion

Synoptic situation: Prior to windstorm event in the

eastern coast of Korean peninsula at 2100 LST, October 27, high pressure system with central pressure 1024 hPa ~ 1025 hPa was present from northeastern Mongolia extending to Winan province in the southwestern China. On the other hand, a low pressure of 1006 hPa was located in the northeastern China passing by northwestern Korean peninsula and extending to the Yellow Sea (Fig. 2a). Atmospheric pressure patterns typically showed the locations of a high pressure in the west and a low pressure in the east. Whole Korean peninsula is underneath low pressure system, which directly affected weather situation over the Korean peninsula.

This low pressure produced northwesterly wind or northerly wind in the west of cold front and supplied cold dry air from northern China into the northwestern Korean peninsula. Oppositely it produced southerly and southwesterly wind in the east of the cold front and induced relative warm moist air from the open sea into the Korean peninsula, showing a thick cloud band on GOES-9 IR satellite image (Fig. 3a). As shown in surface weather map and GOES-9 IR satellite image, before the passage of cold front through Gangneung city at 1800LST and 2100 LST, October 27, wind at the city was southerly or southwesterly of less than 5 m/s near Mt. Taegulyang in the west of Gangneung city and 3 m/s in the city.

However, as the low pressure system continuously moved eastward, especially intruding into the East Sea at 0900 LST, October 28, this low pressure center was located in the coastal sea of northeastern Korean peninsula and it was intensified under meso-scale convection over the sea surface like cyclogenesis, appearing in the narrow displaced isobaric contours on a surface map and producing a strong wind in the mountainous coastal region and the intensified low pressure produced a windstorm over than 13.3 m/s in Mt. Taegulyang at 1200 LST, October 28. As the low pressure intruded into the East Sea, cold front also passed by Gangneung city and observed surface winds on the mountain and coast in the study area were changed westerly with a directional range from 250^0 to 290^0, similarly to calculated winds (Figs. 2b and 3b).

Wind field: Before windstorm was not detected on the mountain and coast in the study, low pressure pattern and cold front generated northwesterly wind or northerly wind in the west of the front formed in the northwestern Korean peninsula, but southerly and southwesterly wind prevails in the east of the front. Observed winds at Mt. Taegulyang and Gangneung city, just before cold front passage across the city at 0600 LST, October 28 were southerly at 1.7 m/s to 3.4 m/s (6.4 m/s to 10.7 m/s at Mt. Taegulyang at an altitude of 865 m height to the west) with a directional range from 200^0 to 250^0 (250^0 to 270^0).

Numerically simulated surface winds were also southerly at 2.0 m/s to 10.2 m/s, similar to the observed ones. As the low pressure system was intensified in the East Sea at 1200 LST, October 28, narrow displaced isobaric contours appeared on a surface map and produced a strong wind in the mountain and coastal region. Since cold front had already passed trough the study area at this time, the previous southerly and southwesterly winds changed to westerly wind and the wind strengthened to more than 9 m/s at the city (K) and 13 m/s near Mt. Taegualyang (T) in the west of the city.

As shown in figure 5a at 2100 LST, October 27, before cold front across the coastal region, major streamline band at 850 hPa level lay on the central Korean peninsula, that is, the northern part of the Gangneung coastal region and cold dry air coming from central Mongolia passed through northeastern China, the Yellow Sea and Gangneung city. As the city (black triangle) was located a little bit away from both major streamline band in fig. 5a and colorful dark area with isotach greater than 25 kts, wind speed at the city was less than 25 kts and no occurrence of windstorm was expected in the study. However, at 0900 LST, October 28, the city was located in both major streamline band in fig. 5b and colorful dark area with isotach greater than 25 kts, wind speed at the city was greater than 25 kts, resulting in the occurrence of windstorm.

From night on October 27 until the next day morning on October 28, synoptic southerly wind changed into downslope westerly wind passing over mountain terrain with steep dropoff in elevation (orography) and combined with land breeze, becoming a strong westerly windstorm in the mountainous coast (Fig. 4). Simultaneously, as synoptic westerly wind blew to the mountain top in the west of the coastal city and began to move down along the eastern slope of the mountain, it was associated with mountain-land breeze generated by both nocturnal cooling of the ground surface and steep mountain terrain, resulting in an intensified strong downslope wind like Katabatic wind or windstorm.

Thus, this downslope windstrom produced the propagation of internal gravity waves with a hydraulic jump motions bounding up and down over the coastal basin and sea such as blocking in the lee side of Mt. Taegulyangas in fig. 6. Calculated Froude numbers were 1.0 near the mountain top and 1.6 in the downwind side, Gangneung coastal city, respectively. Furthermore, when this wind storm passes by the coastal basin, much shallower nocturnal surface inversion layer than daytime convective atmospheric boundary layer could also make a contribution of the increase of surface wind speed. As air flow under shrunken nocturnal surface inversion could be fast, the shrunken of atmospheric boundary can be significant to induce the formation of windstorm.

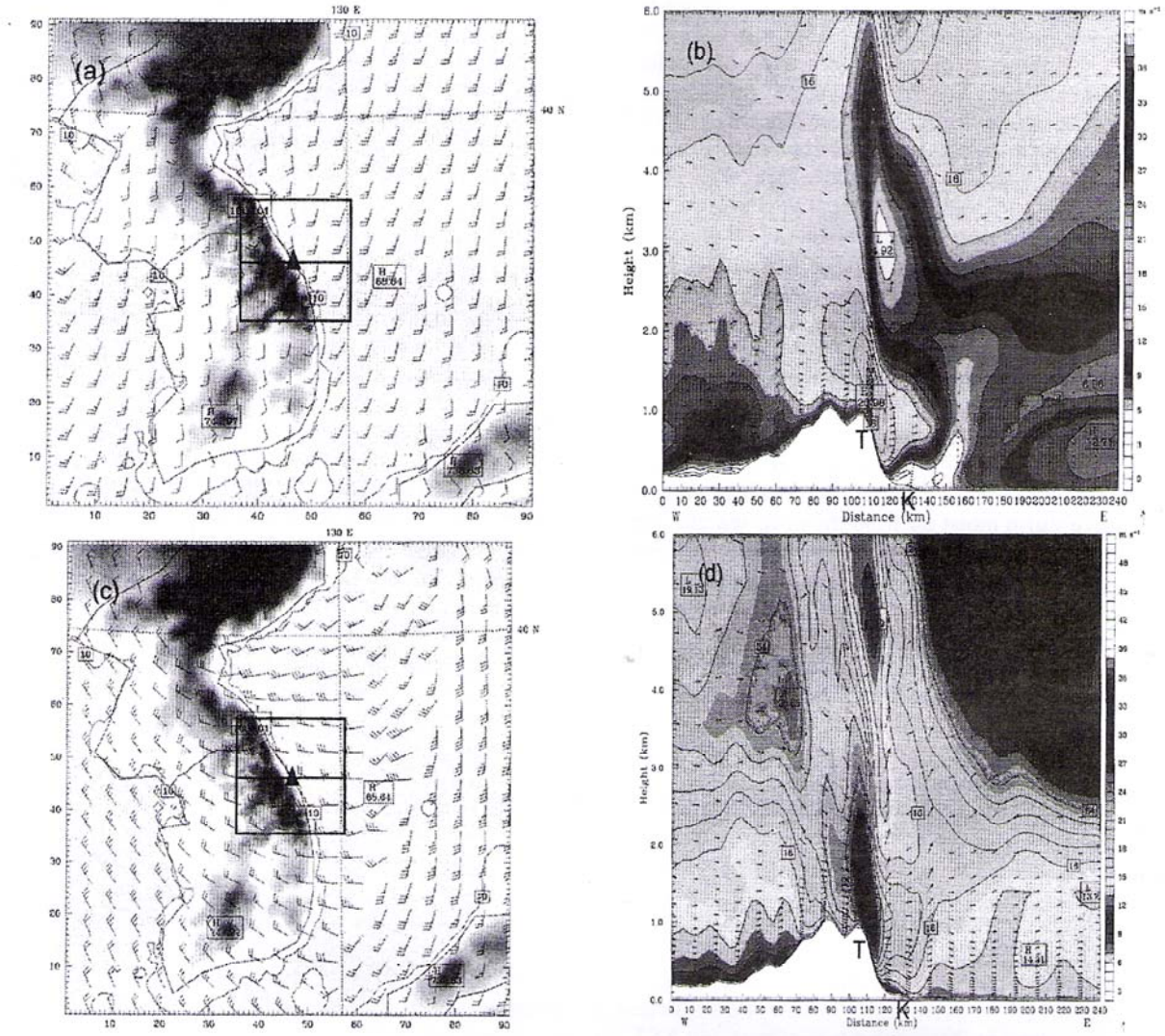

Figure 4: (a) Surface wind (m/s; full bar-5m/s) in the second coarse-mesh domain with a 9 km horizontal resolution and (b) vertical profile of horizontal wind in a box (fine-mesh domain with a 3 km horizontal resolution) on a horizontal line in (a) at 2100 LST, October 27. Triangle denote Gangneung city. (c) and (d) are the similar to (a) and (b), except for 1200 LST, October 28. T and K denote Mt. Taegulyang (865 m) and Gangneung city (20 m). Wind speeds at T and K were 4.9m/s, 1.7m/s in (b) and 13.3 m/s, 9.5 m/s in (d) respectively

Response of vorticity, 500 hPa height change, and 850 hPa temperature change to wind field: Reed and Sanders[21], Reed[22], Sanders and Gyakum[23] and Reed and Albright (1986)[24] insist that progressive troughs (ridges) of upper tropospheric cold low at 500 hPa level having a minimum geopotential height are manifest as groups of height contours open toward the pole (toward the equator), respectively. Holton[13] explains that positive relative vorticity (ζ; 10^{-5}/sec) advection at 500 hPa level is maximum above the surface low, while negative relative vorticity advection is strongest above the surface high. The region of positive relative vorticity inducing convergence of air parcel in the upper level of 500 hPa and its downward motion toward the ground surface matches the region of the negative geopotential tendency ($\partial\Phi/\partial t$; m/day), where atmospheric depth at 500 hPa should be vertically shrunken.

According to Bernoulli theory[25], velocity is inversely proportional to vertical cross sectional area. Thus, much shrunken atmosphere in a certain area produces a strong channel flow, resulting in a possibility of strong wind storm and vice versa. Thus, in general, cyclogenesis or cyclonic flow by cold low in the upper level produces downstream flow toward 850 hPa level and finally reaches the ground surface, which appears in the narrow displaced contours of isobar near the ground surface and the narrow isobaric lines can produce strong surface geostrophic winds.

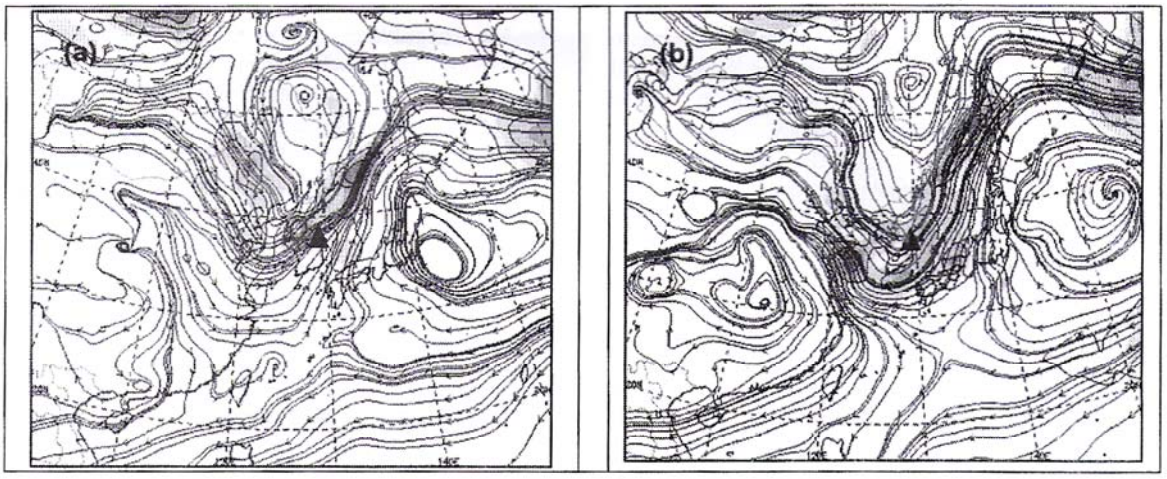

Figure 5: (a) Streamline and isotach at 850 hPa level at 2100 LST October 27, 2003 and (b) 0900 LST October 28. Thin line and colorful dark area denote streamline and isotach greater than 25 kts. Triangle denotes Gangneung city. Wind speed near Gangneung city in (a) was less than 25 kts (no occurrence of windstorm in the study area) while the speed in (b) was greater than 25kts (occurrence of windstorm)

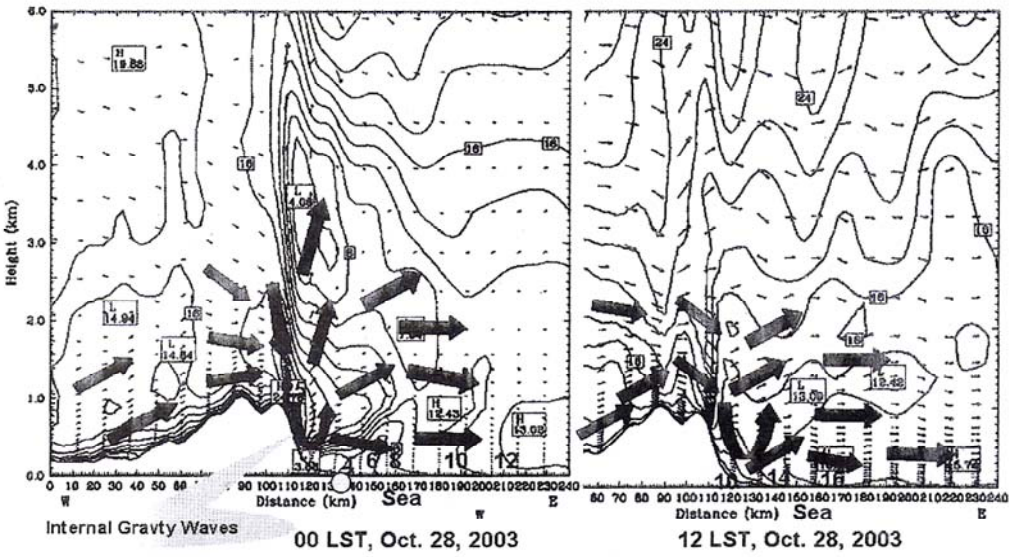

Figure 6: Schematic profile of wind circulations at 0000LST and 1200LST, October 28, 2003. Internal gravity waves with a hydraulic jump motion were found in the lee side of Mt. Taegullyang and Gangneung city

Oppositely, the region of negative relative vorticity, which induces air parcel to be upward from the ground surface to the upper level also matches the region of the positive geopotential tendency, where atmospheric depth at 500 hPa should be vertically expanded. In general, the cold front of surface low-pressure does not directly exist underneath the trough of the upper cold low, showing the location of upper low tilted westward.

It means that the trough of the upper cold low is the left hand side from the tail of cold front. Sometimes, it directly exists underneath the upper trough, resulting in more intensified surface low-pressure. In figs. 7a and 8a, at 21 LST, October 27, before windstorm event in the Gangneung coastal region, maximum positive relative vorticity area at 500 hPa level (dark colorful area) of 22 $x10^{-5}$/sec calculated by the numerical model lay in the northeastern China. This maximum positive vorticity induced convergence of air parcel in the upper level of 500 hPa and resulted in the maximum downward motion of air parcel toward the ground surface. This area also matched the region of the maximum negative geopotential tendency of - 199 m/day (dark colorful area), where atmospheric depth at 500 hPa should have a vertically maximum shrunken (Fig. 9). On the other hand, maximum negative vorticity area (white color area) of - 10 $x10^{-5}$/sec was

found near the northeastern Mongolia, where maximum upward motion of air parcel toward the upper level occurred. This area also matched the region of the maximum positive geopotential tendency (250 m/day), where atmospheric depth at 500 hPa should have a vertically maximum expansion. At this time, in the study, negative vorticity of 9 $x10^{-5}$/sec in fig. 7a and positive geopotential tendency of 50 mm/day in fig. 8a were found near the study of Korea, where upward motion of air parcel from the ground surface to the upper level and vertical expansion of lower atmosphere from the surface to the 500 hPa level should be expected. From Bernoulli application, the expanded atmosphere depth could result in low wind speed in the study area (Fig. 3). As simultaneously, 850 hPa temperature change for 24 hours increased to 2^0C/day in fig. 10a, the lower atmosphere could be expanded vertically. At 2100 LST, cyclonic flow by cold low in the upper level such as positive relative vorticity and negative geopotential tendency producing downstream flow appeared in the left hand side of cold front in fig. 2a

As times went on, on the other hand, at 09 LST, October 28, after the cold front passed by the Gangnerung city, positive relative vorticity induced downward motion of cold air from 500 hPa level toward the ground surface with a decreasing rate of - 6^0C/day at 850 hPa level and simultaneously, negative geopotential tendency line (-160m/day) lay on the study area where the atmospheric depth of 500 hPa level to the ground surface should be much shrunken vertically (Figs. 2b, 3b, 7b, 8b and 10b). These kinds of atmospheric processes near the study area resulted in merging of streamlines with higher speed more than 25 kts of isotach at 850 hPa level and produced the formation of strong surface wind speeds more than 9m/s in the Mt. Taegulyang and Gangneung city (Figs. 5b and 6b) Under this circumstance, from previous night at 2100 LST, October 27 until the next day morning, October 28, synoptic southerly wind changed into downslope westerly wind passing over the steep mountain terrain toward the eastern coastal region and combined with land breeze, becoming a strong westerly windstorm in the mountainous coast (Fig. 4b). As the centers of maximum positive vorticity and maximum negative geopotential tendency approached the coastal near noon on October 28, surface wind under the downward motion of cold air toward the ground surface and the compressed atmospheric depth should be more intensified. As shown in fig. 6, the downslope windstrom produced internal gravity waves with a hydraulic jump in the lee side of the mountain and over the coast.

Furthermore, stable nocturnal surface inversion was developed due to cooling of the ground surface and air parcel inside the stable layer merged to the ground surface. Stable layer near the ground surface might also make a significant contribution to the increase of the surface wind speed, to some extent. Shortly after the cold front passage across Gangneung city, cold air might compress the depth of nocturnal surface inversion layer and the shrunken inversion layer could cause the increase of wind speed at night. Near noon, even though a daytime convective boundary layer was developed with more increased depth than nocturnal surface inversion layer, the shrunken atmosphere behind cold front across the study area under the strong downward motion of cold air behind cold front across the study area could still produce a strong surface wind, resulting in the possibility of the formation of daytime windstorm.

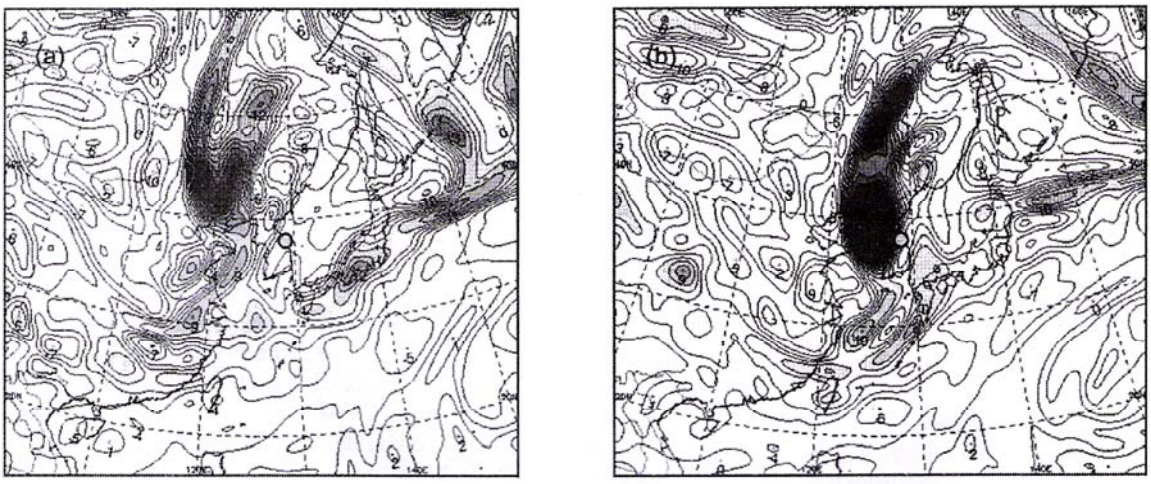

Figure 7: Relative vorticity (10^{-5}/sec) at 500 hPa at (a) 21 LST, October 27, 2003 and (b) 09 LST, October 28. White area denotes negative vorticity (upward motion) and dark area, vice verse. A small circle denotes Gangneung city. As the centers of maximum positive vorticity and maximum negative geopotential tendency approached the coastal near noon, October 28, surface wind due to the downward of cold air and the compressed lower atmospheric depth should be more intensified

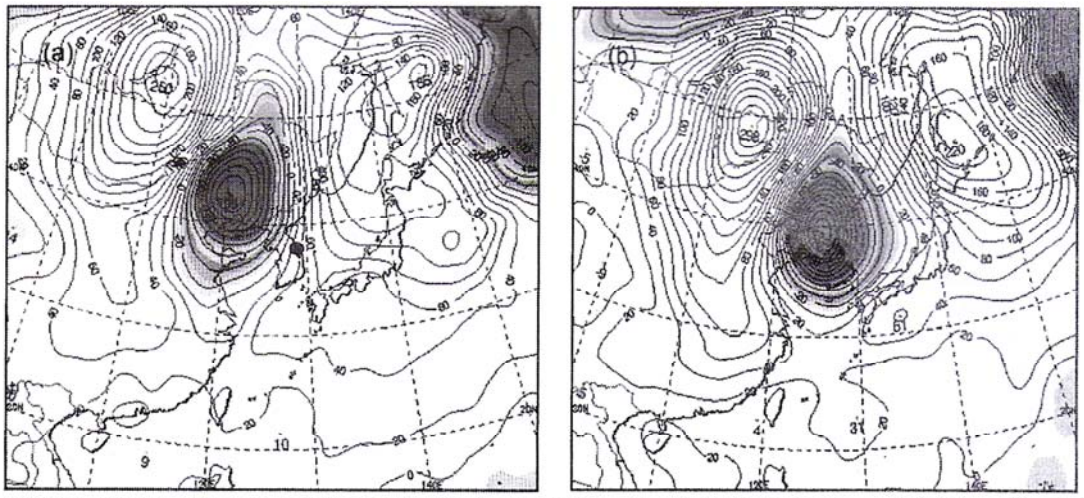

Figure 8: 500hPa height change for 24 hours (m/day) called Geopotential height tendency ($\partial\Phi/\partial t$; m/day) at (a) 2100 LST, October 27, 2003 in the expansion (+ 50m/day) and (b) 0900 LST, October 28 in the shrunken (-160m/day). Shade area denotes the decrease of geopotential height tendency, which implies shrunken of atmosphere and white one, vice verse. A small circle indicates Gangneung city

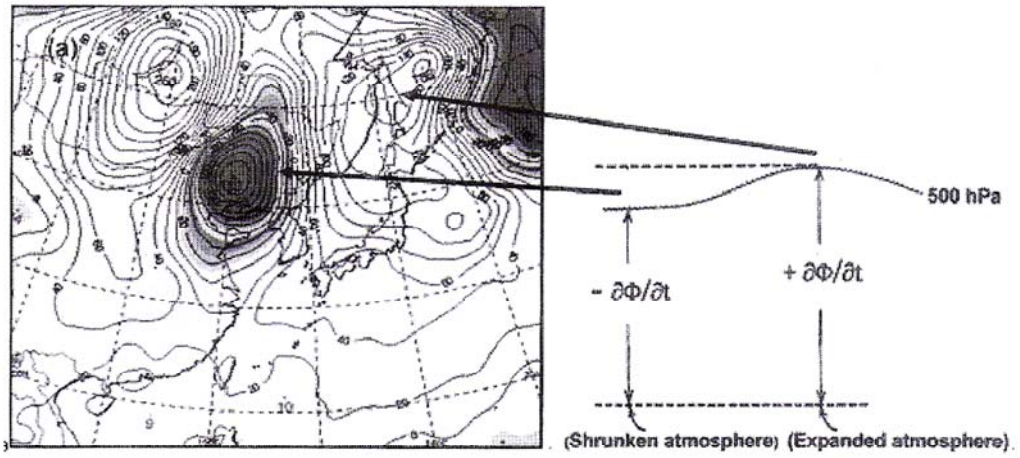

Figure 9: Schematic profile of 500 hPa height change for 24 hours (i.e. geopotential tendency ($\partial\Phi/\partial t$; m/day))

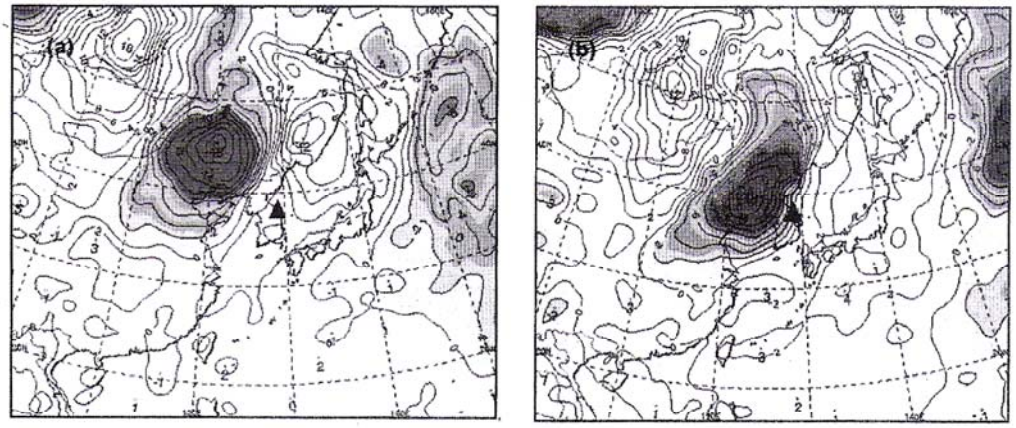

Figure 10: 850 hPa temperature change for 24 hours ($\partial C/\partial t$; C^0/day) at (a) 2100 LST, October 27, 2003 before the occurrence of windstorm in the Ganegneung city and (b) 0900 LST, October 28, around the occurrence of windstorm. Triangle denotes Gangneung city. Dark colorful and white areas denote cooling and warming areas

Response of mountain topographical feature to wind field: When westerly wind is blowing over a mountain barrier, a vertical cross section of the flow may be schematically given in fig. 11. In a homogeneous incompressible fluid, if the flow is adiabatic, each column of air confined between the potential temperature surfaces θo and θo + δθ remains between those surfaces as it crosses the mountain barrier. According to the conservation of potential vorticity, as an air column begins to cross the mountain barrier, its vertical extent decreases. In order to conserve potential vorticity, the relative vorticity must become negative and the air will acquire anticyclonic vorticity, moving southward in the x and y plane[13]. When the air parcel has passed over the mountain barrier, the air column has returned to its original depth and the air parcel in the south of its original latitude. Thus, as Coriolis parameter f with a function of latitude will be smaller, the relative vorticity from potential vorticity conservation equation must be positive, resulting in the air trajectory to have cyclonic curvature.

After the air parcel returned to its original latitude, it still has a northward velocity component and then it continues northward gradually acquiring anticyclonic curvature until its meridional motion direction is reversed. Thus, steady westerly wind blowing over a mountain barrier can produce a cyclonic flow pattern to the east of the barrier followed by a trough and a ridge downstream like a wavelike trajectory in the x, y plane in fig. 11. As soon as synoptic westerly wind begins to pass over the steep mountain barrier, the strong westerly downslope wind enforced by combining with mountain-land breeze depicts a cyclonic flow pattern, resulting in cyclogenesis in the coastal sea and a good condition for the formation of a wind storm.

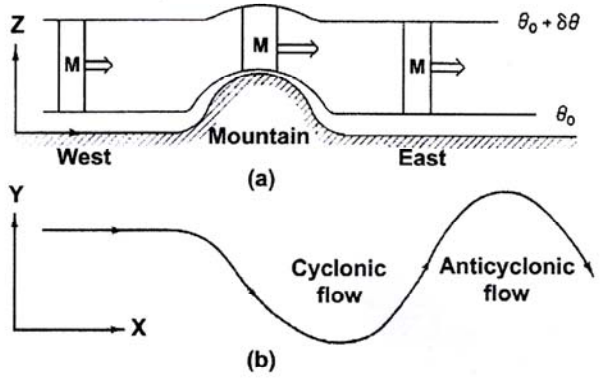

Figure 11: Schematic profile of (a) the depth of air column in the x, z plane and (b) air trajectory in the x, y plane, under westerly wind blowing over a mountain barrier suggested by Holton[13]. As soon as westerly wind passes over a steep mountain barrier, enforced downslope wind depicts a cyclonic flow pattern, resulting in cyclogenesis in the mountainous coastal surface

Comparison of observed and calculated winds: After 48 hours of numerical simulation with FNL meteorological data sets, results of calculated winds were compared with observed ones at Gangwon Regional Meteorological Administration in Gangneung city, Korea. The general tendency of calculated winds well matches with those of the observed, without much discrepancy of each other (Table 1).

Conclusion

Before the occurrence of windstorm event in the eastern mountainous coastal region of Korea, cold front did not pass by this area and winds on the mountain top in the upwind side and at the eastern coastal city were moderate southerly and southwesterly. After cold front had passed trough the study area and moved into the East Sea, the low pressure system was intensified with narrow displaced isobaric contours on a surface weather map and produced a strong wind in the both mountain and coastal region. Moderate southerly and southwesterly winds before windstorm event changed to strong westerly winds and the winds strengthened to m more than 10 m/s in the mountainous coastal region, resulting in the formation of windstorm on the mountain top and in the coastal basin. The downslope windstorm had a hydraulic jump motion bounding up and down in the downwind side coastal basin and depicted lee side internal gravity waves.

Positive relative vorticity at 500 hPa level induced convergence of air parcel in the upper level and the upper convergence induced downward motion of air parcel toward the ground surface. The region of positive vorticity well matched the region of the negative geopotential tendency, which means the decrease of 500 hPa geopotential height for 24 hours and there atmospheric depth at 500 hPa should be vertically shrunken. Before the occurrence of windstorm event in the study area, negative vorticity at 500 hPa level and positive geopotential tendency were found. In this area, upward motion of air parcel from the ground surface to the upper level and vertical expansion of lower atmosphere from the surface to the 500 hPa level should be expected. As Bernoulli theory implies the velocity of a channel flow to be inversely proportional to vertical cross sectional area, the expanded atmospheric depth could result in weak wind speed in the study area and vice versa.

On the other hand, after the cold front passed by the coastal city, positive relative vorticity induced downward motion of cold air from 500 hPa level toward the ground surface with a decreasing rate of - 6^0C/day at 850 hPa level and simultaneously, negative geopotential tendency line (-160m/day) lay on the study area, where the atmospheric depth of 500 hPa level to the ground surface should be much shrunken vertically. This compression of atmospheric layer and downward motion of air parcel in the study area resulted in merging of streamlines with

higher speed more than 25 kts of isotach at 850 hPa level and produced the formation of strong surface wind speeds more than 9m/s in the Mt. Taegulyang and Gangneung city. In addition, when the air parcel has passed over the mountain barrier, the air column has returned to its original depth and the air parcel in the south of its original latitude. As Coriolis parameter is smaller and the relative vorticity due to conserving potential vorticity must be positive, an air trajectory should have cyclonic curvature to cause cyclogenesis and wind speed increase downwind side. Under this circumstance, after the cold front passage across the study area, previous moderate synoptic southerly wind changed into downslope westerly wind as it passed over the steep mountain terrain toward the eastern coastal region. Then the westerly downslope wind combined with mountain-land breeze became a strong westerly windstorm in the mountainous coast, resulting in internal gravity waves with a hydraulic jump in the lee side of the mountain and over the coast.

At night, as stable nocturnal surface inversion was developed due to cooling of the ground surface and air parcel inside the stable layer merged to the ground surface, shallower nocturnal surface inversion layer could more intensify the westerly downslope wind near the surface, resulting in a significant contribution to the increase of the surface wind speed. Simultaneously, after cold front passage across the coastal city, downward cold air from the upper level toward the ground surface could further compress the depth of nocturnal surface inversion layer and produce the increase of the wind speed. Even though daytime convective boundary layer was developed with more increased depth than nocturnal surface inversion layer, the shrunken atmospheric boundary layer behind cold front passing across the study area could still cause the increase of wind speed, resulting in daytime windstorm near noon in the study area. From this result, it may be easy to predict a windstorm for both nighttime and daytime, which has frequently caused vast economical loss due to windstorm disaster in the mountainous coastal region.

Acknowledgement

This work was funded by the Korea Meteorological Administration Research and Development Program under Grant CATER 2006-2308-"Generation mechanism and prediction of wind storm in the mountainous coast".

References

1. Eom J., Analysis of the internal gravity wave occurrences of April 19, 1970 in the Midwest, *Monthly Weather Review*, **103**, 217-226 (**1975**)

2. Anthes R.A., Numerical prediction of severe storms-certainty, possibility or dream, *Bullet American Meteorological Society*, **57**, 423-43 (**1976**).

3. Anthes R.A., Kuo Y.H., Benjamin S.G. and Li Y.F., The evolvation of the meso-scale environment of severe local storms: Preliminary modeling results, *Monthly Weather Review*, **110**, 1187-1213 (**1982**)

4. Bosart L.F. and Seimon A., A case study of an unusually intense atmopsheric gravity wave, *Monthly Weather Review*, **116**, 1857-1886 (**1988**)

5. Kanak J., Benko M., Simon A. and Sokol A., Case study of the 9 May 2003 windstorm in southwestern Slovakia, *Atmospheric Research*, **83**, 162-175 (**2007**)

6. Anderson O.J., The katabatic wind field and nocturnal inversions in valleys: A 2-dimensional model (Report No. 1), Department of Meteorology, University of Bergen, Norway (**1981**)

7. Pielke R.A., Mesoscale meteorological modeling, Academic Press, 612 (**1984**)

8. Hunt J.C. and Simpson, J.E., Atmospheric boundary layer over nonhomogeneous terrain, Elsevier, Amstrerdam (**1982**)

9. Arya S.P., Introduction to micrometeorology, Academic Press, 307 (**1988**)

Table 1
Comparison of calculated wind (m/s) and direction (^{0}; ( )) to observed one at (a) Mt. Taegulyang (T) in the upwind side and (b) Gangneung city from October 27-28, 2003

Date	Comparison	1500	1800	2100	0000	0300	0600	0900	1200	1500
(a) 10/27~10/28 (T)	Observed	6.1 (2.50)	4.7 (250)	4.9 (270)	5.3 (250)	7.3 (270)	9.0 (270)	10.3 (270)	13.3 (270)	13.2 (270)
	Calculated	5.5 (250)	4.5 (240)	5.2 (270)	5.5 (250)	7.5 (270)	10.0 (280)	10.8 (260)	13.5 (270)	13.8 (270)
(b) 10/27~10/28 (K)	Observed	2.0 (110)	4.0 (250)	2.2 (250)	1.0 (230)	1.2 (230)	2.9 (270)	5.3 (250)	9.5 (250)	5.8 (270)
	Calculated	2.0 (120)	4.0 (260)	2.5 (250)	1.5 (240)	1.5 (240)	3.5 (270)	6.2 (260)	10.2 (250)	6.0 (270)

10. Choi H., Persistent high concentration of ozone during windstorm conditions in southern Korea, *Meteorology & Atmospheric Physics*, **87**, 93-107 (**2004**)

11. Anthes R.A., The development of asymmetries in a three-dimensional numerical model of the tropical cyclone, *Monthly Weather Review*, **100**, 461-476 (**1972**)

12. Palmieri S., Teodonio L., Siani A.M. and Casale G.R., Tropical strom impact in Central America, *Meteorological Applications*, **13**, 21-28 (**2006**)

13. Holton J.R., An introduction to dynamic meteorology, fourth edition, Academic Press, 535 (**2004**)

14. Hellin J. and Haigh, M.J., Rainfall characteristics of tropical storm Mitch in southern Honduras, *Weather*, **54** (11), 350-359 (**1999**)

15. Changnon S.A., Pielke Jr, R.A., Changnon D., Sylves R.T. and Pulwarty R., Human factors explain increased losses from weather and climate extremes, *Bulletin American Meteorological Society*, **81**, 437-442 (**2000**)

16. Woo W.C., Tse S.M. and Lam H., Significant rain in Hong Kong associated with distant tropical cyclones over the South China Sea, Reprint 752, Guangdong-Hong Kong-Macau Seminar on Meteorological Science and Technology, Zhongshan, China, 21-23 January 2008 (**2008**)

17. Knauss J.A., Introduction to physical oceanography, Waveland Press, Inc., 320 (**2009**)

18. Choi H., Cold sea outbreak near Cheju Island, Korea by strong wind and atmospheric pressure change under typhoon Rusa, *Disaster Advances*, **3 (1)**, 32-41 (**2009**)

19. Choi H., Choi, D.S. and Choi M.S., Heavy snowfall by orography and wind shift in cold front crossing Korean eastern coast, *Disaster Advances*, **2**(4), 48-60 (**2009**)

20. Cheung T.C. and Chan P.W., Improving wind and rain simulations for tropical cyclones with the assimilation of Doppler radar data, Reprint 835, 10th Annual WRF Users' Workshop, 23-26 June 2009, Boulder, CO, USA (**2009**)

21. Reed R.J. and Sanders F., An investigation of the development of a mid-tropospheric frontal zone and its associated vorticity field, *Journal of Meteorology*, **10**, 338 (**1953**)

22. Reed R.J., Cyclogensis in polar air stream, *Monthly Weather Review*, **107**, 38-52 (**1979**)

23. Sanders F. and Gyakum J.R., Synoptic-dynamic climatology of the "bomb", *Monthly Weather Research*, **108**, 1589 (**1980**)

24. Reed R.J. and Albright M.D., A case study of explosive cyclogensis in the Eastern Pacific, *Monthly Weather Review*, **114**, 2297-2319 (**1986**)

25. Roberson J.A. and Crowe C.T., Engineering fluid mechanics, second edition, Houghton Mifflin Company, 149-159 (**1976**).

(Received 21st December 2009, accepted 20th February 2010)